# $C_{60}$ Exciton Quenching near Metal Surfaces

Klaus Kuhnke, René Becker, Maximilian Epple, and Klaus Kern
*Institut de Physique Expérimentale, EPF Lausanne, CH-1015 Lausanne, Switzerland*
(Received 2 June 1997)

Employing metal-alkanethiol-$C_{60}$ sandwich structures we studied the $C_{60}$ exciton lifetime as a function of distance (1–3 nm) to a metal. Based on the order and compactness of the self-assembling thiol layer a uniform separation of $C_{60}$ and metal is achieved. The $C_{60}$ exciton lifetime is measured by pump and second harmonic probe spectroscopy. Even at distances as small as 1 nm classic damping mechanisms prevail, and no evidence for additional decay channels is obtained. For Au and Ag substrates we find a predominance of energy transfer to bulk and to surface, respectively. [S0031-9007(97)04303-2]

PACS numbers: 73.90.+f, 33.50.Hv, 42.65.–k, 61.46.+w

Energy transfer from an excited state to an energy acceptor is of fundamental importance in physics and chemistry. The classic example is the nonradiative damping of a dipole (e.g., an electronically excited molecule) outside a metal surface [1,2]. In a simple picture a dynamic dipole creates eddy currents within the metal which lead to the dissipation of the dipoles energy. The key result, the decrease of the nonradiative transfer rate with the cube of the metal-dipole distance, was confirmed in numerous experiments probing the decay of excited molecules separated from metallic substrates by dielectric spacers [3–7].

These experiments were, however, limited to metal-molecule distances larger than $\approx 3$ nm. The fundamental question down to which distance classic electromagnetic theory is still valid and where it breaks down could not be addressed. Indeed, in close proximity substantial deviations from the classical picture due to the onset of tunneling are expected. In this Letter we present an experimental study of excited state decay near a metal. The distance range from 3 nm down to 1 nm is probed quantitatively. The experimental data for the $C_{60}$/alkanethiol/Au,Ag sandwich structures demonstrate that even at distances as small as 1 nm classic electromagnetic decay prevails.

The distance dependence of excited state lifetimes can be measured only if a significant number of probe molecules is positioned at a well defined distance from the metal substrate. This has to be done with increasing absolute precision when the distance is reduced. Inhomogeneities and defects can substantially affect the results. Up to date multilayers of Langmuir-Blodgett films and rare gases were employed [3–7]. They allow distance control down to about 3 nm. The rare gas layers have the disadvantage of preparational difficulty in the generation of uniform and flat layers and potential problems with interdiffusion, while the Langmuir-Blodgett technique involves building blocks which are too thick to allow a fine-tuning of distance. The ultimate length scale of distance variation is the interatomic distance ($\approx 0.1$ nm). If spacers of rigid atomic chains are employed which are oriented perpendicular to the surface, small units can be added or removed in the chain, allowing a distance adjustment with a precision of less than 0.1 nm.

We present a model sandwich system which exhibits such ideal spacer layer properties. Alkanethiol spacer layers which self-assemble from solution are known to form dense and uniform adlayers on many metal surfaces [8]. The molecules adsorb with the hydrocarbon chain nearly perpendicular to the surface and can be commercially obtained with different chain lengths. Avoiding the difficulties due to the different properties of chains with even and odd numbers of carbon atoms, the spacer thickness can easily be varied by multiples of —$(CH_2)_2$— groups, i.e., by multiples of 0.2 nm. We further demonstrate for our sandwich system that alkanethiols have a negligible influence on the excited state lifetime of the probed molecules which physisorb on the functional methyl group of the thiol.

The probed molecule in the sandwich system is the fullerene $C_{60}$ which was demonstrated to exhibit a transient reduction of optical second harmonic generation (SHG) for pump densities of only a few $\mu J/cm^2$ [9]. The lifetime measurement is performed as follows: A UV (3.49 eV) pump pulse of 25 ps duration excites the $C_{60}$ film thus defining time zero. After a variable delay the pulse is followed by an IR (1.17 eV) probe pulse (35 ps) which generates a second harmonic (2.35 eV) signal at the sample. $C_{60}$ is transparent at the probe beam wavelength. At any delay the SH signal reduction is (for sufficiently weak excitation) proportional to the density of excited states. Thus, from the SH signal as a function of the pump-probe time delay the decay rate of the excited electronic state is directly obtained. The signal is interface sensitive which allows one to monitor lifetimes even at varied interfaces. In an earlier study the excited state was determined to be a low-lying excitonic state [9]. SHG thus gives us the opportunity to monitor these states without employing fluorescence or phosphorescence measurements. The lowest singlet exciton decays in approximately 1.2 ns [10] to the lowest triplet exciton which has a lifetime of the order of 100 $\mu$s [11]. We find that the SH signal is reduced in faster than 30 ps and recovers with a time constant which must lie between 20 ns and 20 ms.

 0031-9007/97/79(17)/3246(4)$10.00 

We conclude that singlet and triplet excitons must both contribute to SH quenching.

The experimental geometry is shown in Fig. 1. Pump and probe beams are incident at an angle of 45° with respect to the surface normal forming a small angle (≈8°) between each other. The SH photons are generated in a narrow beam in specular reflection from the interface. The geometry and the small intensity of the pump beam exclude the detection of pump-probe difference frequency generation in the measurements.

The preparation of well ordered thiol monolayers on Au and Ag surfaces is described in detail elsewhere [12]. Pure $C_{60}$ powder (99.9%) preheated in high vacuum for some 50 h is evaporated at 680 K from a Knudsen cell onto the thiol layer to obtain thin films of less than 20 nm thickness. The sample is transferred to a high vacuum ($10^{-6}$ mbar) chamber in which the experiments are performed at room temperature.

In Fig. 2 a scanning tunneling microscopy (STM) image for a submonolayer $C_{60}$ coverage is shown. The Au substrate exhibits flat terraces on a 100 nm scale. The pits of one Au layer depth are due to the etching of the substrate during thiol self-assembly. Like the terraces, the etching pits are covered by the thiol layer [12]. The dark, parallel lines represent domain boundaries which separate highly ordered molecular domains [12]. The bright spots in the image are the $C_{60}$ molecules which are mobile enough to reach preferential adsorption sites at thiol domain boundaries or in the etching pits. This strongly suggests that $C_{60}$ physisorbs on the thiols and does not chemically react with the methyl group. This conclusion is supported by the fact that the $C_{60}$ film can be completely removed by rising in chloroform [13].

Figure 3 shows pump and SH probe transients of $C_{60}$/alkanethiol/Au(111) sandwiches for different alkane chain lengths $n$ adsorbed on Au. The measurements for Ag exhibit equivalent features. The transients exhibit two contributions, one with a long lifetime ($\tau \gg 1$ ns) and a second with a reduced lifetime. Similar to the earlier interpretation of $C_{60}$ thin films on quartz [9], we ascribe the long lived state to the surface of the $C_{60}$ film and the short lived state to its interface with the substrate. Because of the optical properties of Au a significant part of the second harmonic signal at 2.35 eV is due to the Au substrate which results essentially in a signal offset. $\chi_0^{(2)}$ is the second polarizability of the sandwich system at the probe frequency when no excitation is present. We can describe the normalized transient signal by the following formula:

$$\frac{S(t)}{S_0} = \left( \left\{ 1 - \theta(\tilde{t}) \left[ \frac{\Delta\chi^{(2)}_{\text{long}}}{\chi_0^{(2)}} + \frac{\Delta\chi^{(2)}_{\text{short}}}{\chi_0^{(2)}} \exp\left( -\frac{\tilde{t}}{\tau} \right) \right] \right\} \circ R(\tilde{t} - t) \right)^2 . \quad (1)$$

Here, $\theta$ is the Heaviside function [$\theta(t) = 1$ for $t > 0$ and $\theta(t) = 0$ for $t < 0$] and $R$ is a Gaussian function representing the time resolution function of the experiment. The formula is based on the following model: At $t = 0$ the pump beam excites long lived and short lived states which both reduce the second order nonlinear susceptibility $\chi_0^{(2)}$ related to the sample without excitation. $\chi^{(2)}$ is assumed to return to its original value $\chi_0^{(2)}$ by a single exponential decay for the short lived state plus a decaying long lived state, here approximated by a constant. This amplitude function is convoluted with the experimental time resolution $R$ and then squared to obtain the normalized SH intensity.

Figure 4 shows the decay rate $1/\tau$ as a function of the spacer layer thickness obtained by fitting the data with Eq. (1). The results for the Au and Ag substrates are marked by circles and triangles, respectively. The spacer thickness $d$ for thiols adsorbed on Ag is obtained from the formula $d = 5.6$ Å + (1.3 Å)$n$ [8], where $n$

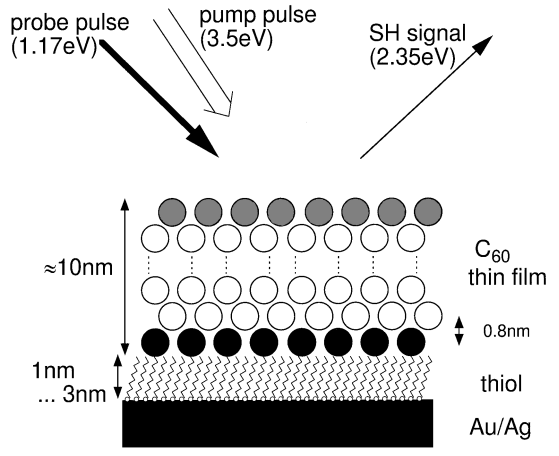


FIG. 1. Schematic representation of the metal/alkanethiol/$C_{60}$ sandwich structure and the beam geometry for pump and SH probe transient spectroscopy.

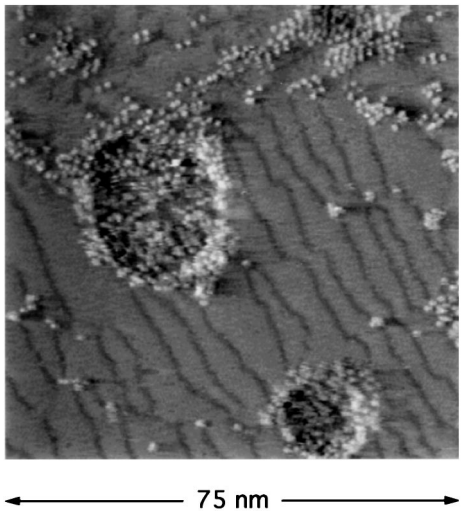


FIG. 2. STM image of the initial stage of growth of $C_{60}$ on decanethiol covered Au(111).

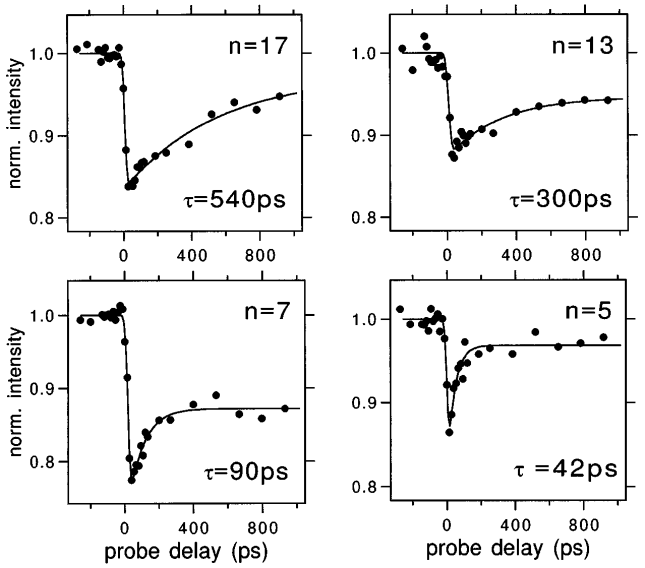


FIG. 3. Pump and SHG probe transients for sandwich structures with Au substrates and different thiol $SH(CH_2)_nCH_3$ chain lengths $n$. The points represent the data, and the dotted lines are fits according to Eq. (1). For each measurement the lifetime $\tau$ of the short lived component is indicated.

is the length of the carbon chain. In the determination of the thickness on Au it was taken into account that the thiol molecules are not adsorbed perpendicularly as on Ag but tilted by 25°. The thiol layer itself has a negligible effect on the observed decay: The coupling between the exciton and the methyl groups of the thiol to which the $C_{60}$ molecule is physisorbed will not change with the thiol chain length. As we do not observe that the decay rate tends towards a constant value for the thickest spacer layers the transfer rate from the exciton to the thiol must be much smaller than the smallest measured decay rate. From the single exponential decay specifically of the measurements for $n = 5$ and $n = 7$ we conclude that the observed short lived state results from only one $C_{60}$ layer at the interface. Else we should observe, because of the large $C_{60}$ layer distance of 0.8 nm (see Fig. 1), a series of exponentials with distinct time constants, each resulting from a different $C_{60}$ layer. The sensitivity to the immediate interface is a prerequisite for a precise evaluation of the dependence of the rate constant on $C_{60}$-metal distance.

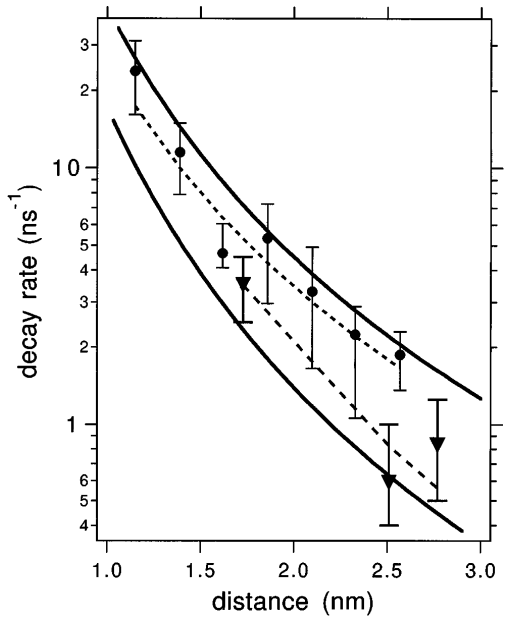


FIG. 4. Decay rate $1/\tau$ as a function of thiol layer thickness. The circles and triangles represent the measurements for Au and Ag substrates, respectively. The dotted lines are algebraic fits according to Eq. (2) while the solid lines are obtained according to Eq. (3) (see text). The upper lines refer to measurements of samples with Au substrates, and the lower lines refer to Ag samples.

The data in Fig. 4 were fitted in two ways. First, a power-law fit

$$\tau_{\text{eff}}^{-1} = \alpha d^{-m} \tag{2}$$

allows one to determine the multipole order of the coupling and the dimensionality of the acceptor system by means of the positive integer $m$; $\alpha$ is a proportionality constant which will not be analyzed. An electric dipole to bulk transfer, e.g., is characterized by $m = 3$, a magnetic dipole to bulk transfer by $m = 1$, and an electric dipole to surface transfer will have $m = 4$ [2,14]. Best fits for the Au and Ag surfaces according to Eq. (2) are shown as dashed lines in Fig. 4. The best fit exponents are $m = 2.9\ (+0.7/-0.5)$ for Au and $m = 3.9\ (+0.6/-0.9)$ for Ag. The results already indicate that the transfer is dominated by electromagnetic decay. No evidence for tunneling contributions are observed. In the case of Ag the transfer to the surface is more important while Au exhibits transfer to electrons in the bulk.

The second fit (solid lines in Fig. 4) allows a quantitative analysis based on the analytic expression for the decay rate developed by Persson and Lang [15],

$$\tau_{\text{eff}}^{-1}(d) = \tau_{\infty}^{-1}\left(1 + \frac{1}{d^3}\frac{1}{2k^3}\,\text{Im}\left\{\frac{\varepsilon_m(\omega) - \varepsilon_1}{\varepsilon_m(\omega) + \varepsilon_1}\right\} + \frac{1}{d^4}\frac{1}{4k^3}\,\xi(r_s)\,\frac{\omega}{\omega_F k_F}\right), \tag{3}$$

which includes in the bracket three terms, corresponding to the free radiation decay, the electric dipole transfer to the bulk metal and to the metal surface. The approximation inherent in the last term is valid for both Au and Ag as $d \gg \omega_f/(\omega k_f) = 0.25$ nm. In (3) $k$ and $\omega$ are the wave vector and the frequency, respectively, of the electromagnetic field generated by the excited state. We can assume that the exciton decay occurs in the $C_{60}$ fluorescence region at $\hbar\omega = 1.7$ eV. $\omega_F$ and $k_F$ are the Fermi frequency and the Fermi wave vector of the metal, respectively, which were taken from [16]. $\xi(r_s)$ is a function discussed in [15] with $\xi(r_s) = 1.2$ for Au and Ag ($r_s = 3$); $r_s$ is the free electron radius. $\varepsilon_1$ is

the permittivity of the thiol layer ($\varepsilon_1 = 2.1$) [8] and $\varepsilon_m(\omega)$ is the (complex) permittivity of the metal at the dipole radiation frequency. The term in brackets is thus completely determined by literature values. The second term in the bracket is due to the bulk absorption and dominates the decay rate for Au substrates even at 1 nm because of the onset of strong interband transitions in the visible. This is in agreement with the observed $d^{-3}$ behavior in this case (Fig. 3). For Ag the second term is much smaller, and the surface term begins to dominate at about 2 nm separation which is reflected in a transition to a $d^{-4}$ behavior. The only unknown parameter in Eq. (3) is the $C_{60}$ exciton free radiation lifetime $\tau_\infty$. By assuming $\tau_\infty = 1.0 \pm 0.5$ $\mu$s we obtain an agreement with the Au and the Ag data (solid lines in Fig. 4). In the case of the Au samples the good agreement demonstrates that the distance dependence is well described by the theoretical model. The data for the Ag substrates appear to be less conclusive. The Ag samples were more difficult to prepare in good quality so that only data for three different thiol lengths could be obtained. These data are, however, consistent with the model both in the absolute rate constant and in the exponent determined by the power-law fit according to Eq. (2). The difference between the Au and the Ag rate constants is slightly smaller than predicted by theory.

As we already discussed, the candidates for the monitored excitonic state are the lowest singlet and triplet states. $\tau_\infty$, however, must be greater than the effective lifetime of an observed state. The small value obtained for $\tau_\infty$ suggests that in this experiment the singlet exciton is observed rather than the triplet exciton. The comparison of $\tau_\infty$ with the effective lifetime of the singlet state of approximately 1.2 ns suggests a fluorescence quantum efficiency of $1.2 \times 10^{-3}$ $(+1.2 \times 10^{-3}/-0.5 \times 10^{-3})$ which, in fact, agrees with the experimental value of $0.7 \times 10^{-3}$ [17].

It is known from the literature that the singlet exciton is of $T_{1g}$ symmetry and its decay to the $C_{60}$ ground state of $A_g$ symmetry is dipole forbidden and takes place via a magnetic dipole transition. This transition multipole, however, would result in a $d^{-1}$ dependence of the decay rate in the case of Au and a $d^{-2}$ dependence at short distances in the case of Ag. The exponents obtained in our study do thus explicitly show that the forbidden transition acquires electric dipole character by intensity borrowing from dipole allowed modes via Herzberg-Teller coupling. This result is also important for the interpretation of resonant second harmonic generation at $C_{60}$ interfaces: By this mechanism forbidden transitions can become electric dipole allowed. Dipole allowed transitions, however, cannot efficiently generate SH radiation in centrosymmetric bulk structures. We thus obtain for such transitions in $C_{60}$ the interesting result that resonant SHG becomes allowed at the interface while it remains forbidden in the bulk. The surface and interface sensitivity of SHG spectroscopy can thus be restored even for forbidden transitions which is remarkable because $C_{60}$ was shown to exhibit substantial SHG bulk contributions [18].

In conclusion, we have shown that thiol spacer layers allow a controlled fine tuning (0.2 nm) of separations in sandwich structures at short distances ($d = 1-3$ nm). The spacer layer does not contribute to the lifetime reduction due to the weak coupling (physisorption). We have further demonstrated that at short distances $>1$ nm the quenching of a $C_{60}$ exciton at a Au surface is still dominated by a $d^{-3}$ dependence which can be ascribed to efficient volume damping due to accessible interband transitions. The result is described by the Persson-Lang model containing only one adjustable parameter which reproduces correctly the known fluorescence efficiency. For a limited number of Ag substrates we find longer lifetimes than for Au samples and a distance dependence which indicates the predominance of surface damping. The distance dependence for both substrates directly confirms that the forbidden exciton decay obtains electric dipole character due to vibronic coupling.


[1] A. Sommerfeld, Ann. Phys. **28**, 665 (1909).
[2] R. R. Chance, A. Prock, and R. Silbey, Adv. Chem. Phys. **37**, 1 (1978), references therein.
[3] A. Adams, R. W. Rendell, W. P. West, H. P. Broida, and P. K. Hansma, Phys. Rev. B **21**, 5565 (1980).
[4] R. Rossetti and L. E. Brus, J. Chem. Phys. **73**, 572 (1980).
[5] A. P. Alivisatos, D. H. Waldeck, and C. B. Harris, J. Chem. Phys. **82**, 541 (1985).
[6] Q. Q. Shu, P. K. Hansma, P. Das, and H. Metiu, J. Lumin. **40/41**, 745 (1988).
[7] F. Balzer and H.-G. Rubahn, J. Electron Spectrosc. Relat. Phenom. **64/65**, 321 (1993).
[8] A. Ulman, *An Introduction to Ultrathin Organic Films* (Academic Press, Inc., Boston, 1991).
[9] K. Kuhnke, R. Becker, and K. Kern, Chem. Phys. Lett. **257**, 569 (1996).
[10] H. J. Byrne, W. Maser, W. W. Rühle, A. Mittelbach, W. Hönle, H. G. von Schnering, B. Movaghar, and S. Roth, Chem. Phys. Lett. **204**, 461 (1993).
[11] H. J. Byrne, in *Physics and Chemistry of Fullerenes and Derivatives*, edited by H. Kuzmany, J. Fink, M. Mehring, and S. Roth (World Scientific, Singapore, 1995), p. 183, and references therein.
[12] O. Cavaleri, A. Hirstein, J.-P. Bucher, and K. Kern, Thin Solid Films **284/285**, 392 (1996).
[13] R. Becker, O. Cavalleri, and K. Kern (unpublished).
[14] H. Kuhn, J. Chem. Phys. **53**, 101 (1970).
[15] B. N. J. Persson and N. D. Lang, Phys. Rev. B **26**, 5409 (1982).
[16] N. W. Ashcroft and N. D. Mermin, *Solid State Physics* (CBS Publishing Ltd., Saunders College, Philadelphia, 1987).
[17] P. A. Lane, L. S. Swanson, Q.-X. Ni, J. Shinar, J. P. Engel, T. J. Barton, and L. Jones, Phys. Rev. Lett. **68**, 887 (1992).
[18] B. Koopmans, A.-M. Janner, H. T. Jonkman, G. A. Sawatzky, and F. van der Woude, Phys. Rev. Lett. **71**, 3569 (1993).